AN INVESTIGATION OF CRACK INITIATION IN SPUR GEARS BASED ON FINITE ELEMENT DYNAMICS ANALYSIS

[1]Amit Zala, [2]Pro.(Dr).Divyang Pandya, [3]Prof.Parth Patel
[1]PG Student, [2]Head of the Department, [3]Assistant Professor
[1]Mechanical Department
[1]LDRP-ITR, Gujarat, India.

Abstract:
Contact fatigue, one of the main failure modes of gear tooth flanks, is caused by repeated compression and shear stress cycles. In this study, the surface and subsurface stresses of gear teeth are investigate during Hertzian theory and the finite element method. The number of loading cycles required for fatigue crack initiation is predicted using method based on the multiaxial fatigue mechanism. Friction is found to shift the distributions of von Mises stress, change the extreme values of the shear stress cycle, and results in low fatigue life. The stresses near the engagement and recess areas a real so found to be greater than the static contact conditions and thus result in low fatigue life, particularly at high speeds. Cracks initiated at the surface may lead to typical life-limiting fatigue failure modes such as pitting and tooth root breakage. Furthermore, the contact load on the flank surface induces stresses in greater material depth and may lead to crack initiation below the surface if the local material strength is exceeded. Over time the sub-surface crack propagation may lead to gear failure referred to as "tooth flank fracture".
Key words: Spur Gear, Finite element dynamics analysis, cracks initiation.

1. Introduction:

The contact fatigue process can be divided into two main stages: initiation of micro-cracks and crack propagation. Initiation of fatigue cracks represents one of the most important stages in which cracks represents one of the most important stages in which cracks can be initiated either on the flank surface or root. The main aim of this study is to predict contact fatigue crack initiation resulting from high stresses or strains during the mesh processes [1-2].
Recently, the finite element method has been increasingly used to simulate rolling and sliding contact, and considerably precise stress results are expected. The worst load condition is often regarded as the condition wherein one pair of teeth carries the full load, and the position in the area around the inner point of a single teeth pair engagement is simulated with the maximum value of contact pressure. Given that the finite element dynamic contact is necessary to investigate stresses at various speeds. Once the stress loading cycles are established, the number of stress cycles required for a fatigue crack to appear can also be determined. Contact fatigue is typically a multiaxial fatigue mechanism, for which several methods, such methods include Theoretical: Hertz theory and Computational: Equivalent stress.[3-4].
In the present study, contact stress analysis and fatigue crack initiation prediction are applied to a pair of spur gears in a high-speed diesel engine. The stresses and numbers of loading cycles required to initiate fatigue cracks at various positions and speeds are investigated [5-9].

2. Fatigue Process:

Contact fatigue is one of the most common failure modes for gear tooth surface and is commonly attributed to the repeated rolling and sliding contact loads. The contact fatigue process and be divided into two main stages: initiation of micro-crack and crack propagation. Initiation of fatigue cracks represents on of the most important stages in which cracks can be initiated either on the most important stages in which cracks can be initiated either on the surface or at some distance under the surface depending on the contact conditions. To predict contact fatigue crack initiation resulting from high stresses or strains during the mesh process.

- Crack initiation is a early development of damage.
- Crack growth is depending of initial crack on shear planes.
- Crack growth defined crack on planes normal to maximum tensile stress.

Fatigue: Crack initiation + Propagation

3. Contact Mechanics:

While Classical Mechanics deals solely with bulk material properties Contact Mechanics deals with bulk properties that consider surface and geometrical constraints. It is in the nature of many rheological tools to probe the materials from "outside". For instance, a probe in the form of a pin in a pin-on-disk tester is brought into contact with the material of interest, measuring properties such as hardness, wear rates, etc. Geometrical effects on local elastic deformation properties have been considered as early as 1880 with the Hertzian Theory of Elastic Deformatio.1 This theory relates the circular contact area of a sphere with a plane (or more general between two spheres) to the elastic deformation properties of the materials. In the theory any surface interactions such as near contact Van der Waals interactions, or contact Adhesive interactions are neglected.
An improvement over the Hertzian theory was provided by Johnson et al. (around 1970) with the JKR (Johnson, Kendall, Roberts) Theory.1 In the JKR-Theory the contact is considered to be adhesive. Hence the theory correlates the contact area to the elastic material properties plus the interfacial interaction strength. Due to the adhesive contact, contacts can be formed during the unloading

cycle also in the negative loading (pulling) regime. Such as the Hertzian theory, the JKR solution is also restricted to elastic sphere contacts.

A more involved theory (the DMT theory) also considers Van der Waals interactions outside the elastic contact regime, which give rise to an additional load. The theory simplifies to Bradley's Van der Waals model if the two surfaces are separated and significantly apart. In Bradley's model any elastic material deformations due to the effect of attractive interaction forces are neglected. Bradley's non-contact model and the JKR contact model are very special limits explained by the Tabor coefficient.

$$\sigma_c = \frac{2P}{\pi bl}$$

$$\text{and } b = \left[\frac{2P(1-\pi^2)\left(\frac{1}{E_1}+\frac{1}{E_2}\right)}{\pi l\left(\frac{1}{d_1}+\frac{1}{d_2}\right)}\right]^{1/2}$$

$$\sigma_c{}^2 = \frac{1}{\mu(1-\mu^2)}\left(\frac{P}{l}\right)\left(\frac{\left(\frac{1}{r_1}+\frac{1}{r_2}\right)}{\left(\frac{1}{E_1}+\frac{1}{E_2}\right)}\right)$$

$$\sigma_c^2 = \frac{1.4\ p_t}{bQd_p \sin\alpha \cos\alpha(1/E_1 + 1/E_2)}$$

$$\sigma_c^2 = \frac{1.4*205}{38*1*39.96*\sin 20 \cos 20\ [\ 1/71000+1/71000]}$$

$$= \frac{287}{1518.48*0.34*0.93*[2/71000]}$$

$$= \frac{287*35500}{480.14}$$

$$= \frac{10188500}{480.14}$$

$$= 145.67\ N/mm^2.$$

4. Geometry and Stress Analysis:

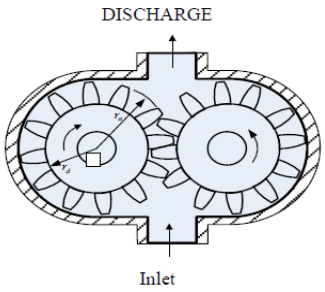

Design parameter:

Discharge specification = 24.55litres/min

Inlet port of diameter = 32mm

Pressure angle = 20◦

Width = 38mm

No. of tooth = 12

Pitch circle diameter = 40 mm.

Circular pitch (Pc) = $\frac{\pi D}{T}$

Where D = diameter of the pitch circle.

T = Number of teeth.

$$= \frac{3.14*40}{12}$$

$$= 10.466 \text{ mm}$$

Module (m) = $\frac{1}{p_c}$

$$= \frac{1}{10.466}$$

$$= 3.33$$

Center of distance (a) = $\frac{m\ (T_1 + T_2)}{2}$

$$= \frac{3.33\ (12+12)}{2}$$

$$= 40.00\ mm$$

5. Modeling of gear:

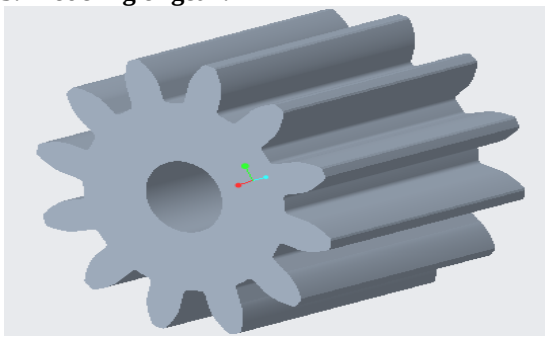

Fig.1 3-D Model Of Spur Gear

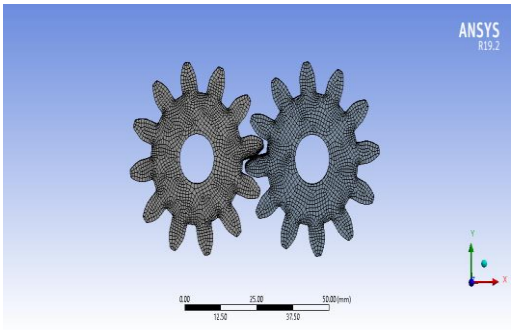

Fig.2 Meshing Of Spur Gear

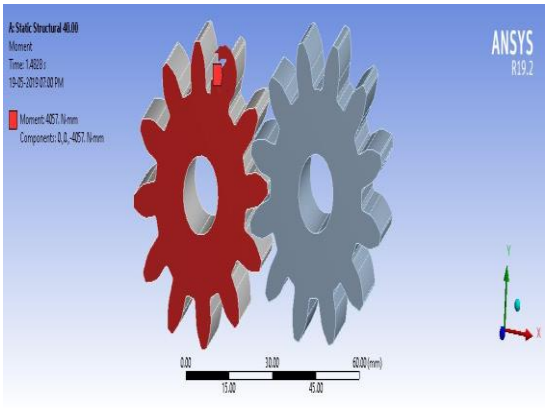

Fig 3 Moment

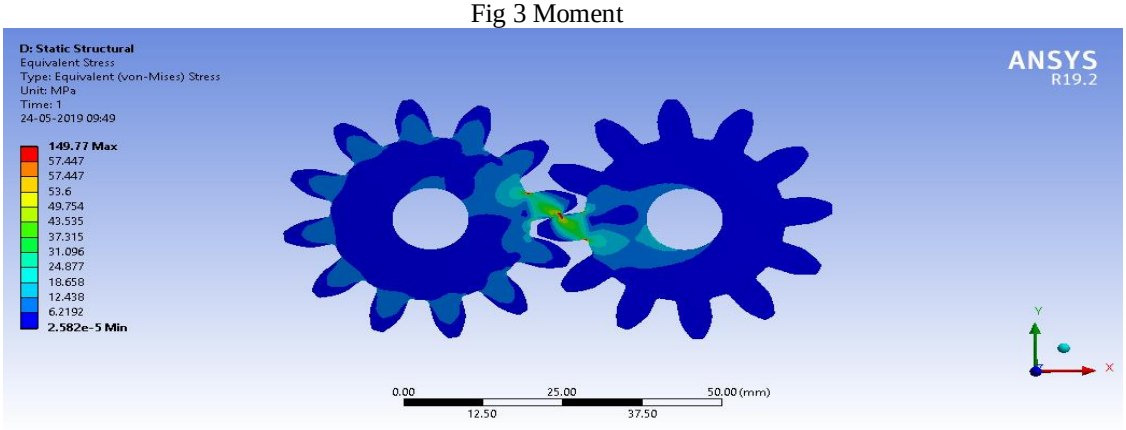

Fig. 4 Equivalent Stress

Left side body is driving spur gear and right hand body is driven spur gear. Following with the frictionless supports to driving gear fixed support to driven gear and moment = 4057 N-mm given to the driving gear, rotates in a clockwise direction. The spur gear provides tangential force, to the gear. Stress at the flank, and stress at the tooth root of spur gear studied in this section. The von Mises stress distribution would be obtained at the contact region and at the root of the spur gear tooth. Figures 4 above present the stress distribution over the gear flank and gear root with aluminium spur gear material. And the maximum stress generation on the spur gear 149.77 N/mm^2. Theoretical Hertzian value after calculation is 145.67 N/mm^2.

$$\% \text{ Error in contact stress} = \frac{149.77 - 145.67}{145.67} \times 100$$
$$= 2.81\%$$

	FEA Value (MPa)	Hertzian Value (MPa)	Difference error (%)
Von Mises Stress	149.77	145.67	2.81

6. Fractures in Spur gear:

Here, we do divide crack propagation into two parts (I) Crack at the root, (II) Crack on the flank of the spur gear. Procedure will be the same for both cracks.

(I) Crack at the root:

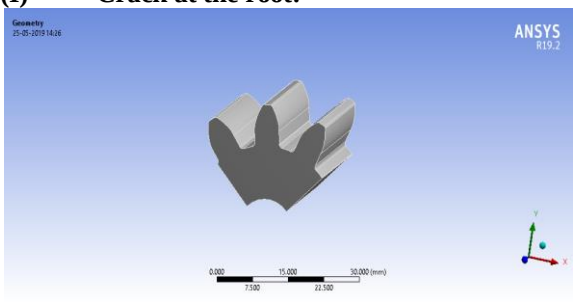

Fig. 5 Gear geometry

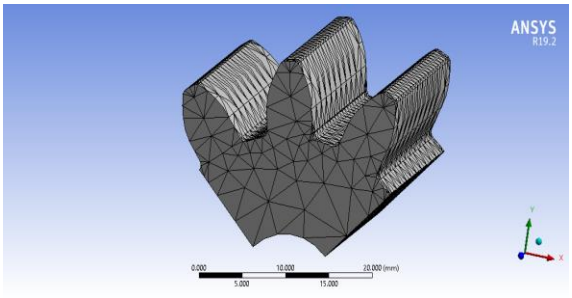

Fig.6 Meshing of spur gear

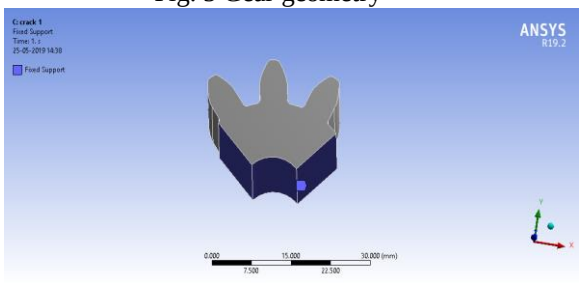

Fig. 7 Fixed Support

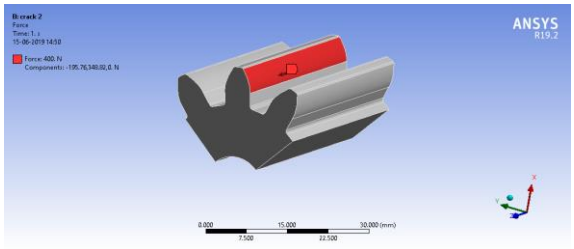

Fig. 8 Force on the flank surface

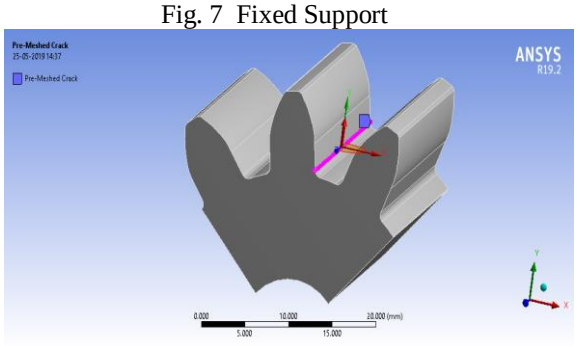

Fig. 9 Pre-Mesh Crack

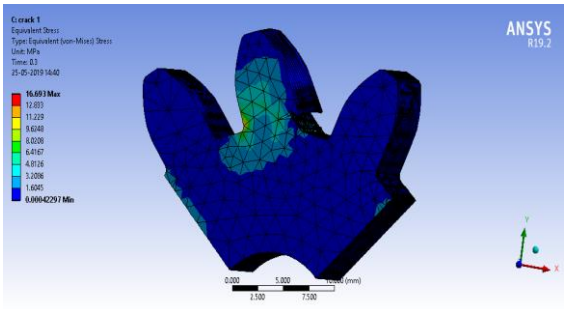

Fig. 10 Fracture in spur gear root

Geometry of the three spur gear teeth of material Aluminium 2024 –T4. For the meshing part choose Tetrahedrons method element order and size – quadratic 3.5mm with physical preference custom (Beta). All the mesh related details shows in Figure. 6. For the analysis, boundary conditions are essential things. In the figure-7 and figure-8. give fixed support to the bottom surface and force should be on the surface of the flank. There value is 400 N. After that for fracture mechanism, using smart crack feature. For that purpose using pre-mesh crack, it need faces node. Face node give by the selecting the face of the crack. All the detail of pre-mesh crack gives in the Figure 9. When compute the result, after the high level of computational power and most amount of time fracture is done and it is easily show in the figure-10. In the above figure-10, fracture happen in region of spur gear root. During the fracture processes change in mesh in every step which is due to custom (Beta) mesh.

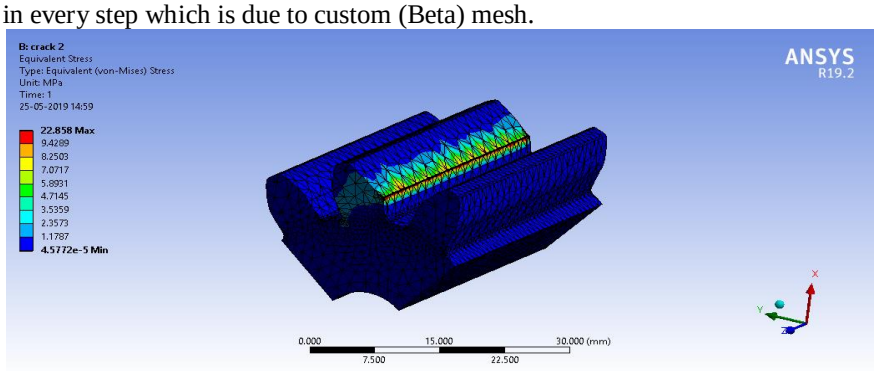

Fig.11 Fracture on the flank surface

The same procedure as mention above for crack at the root of spur gear teeth. Which same follow for the crack on flack surface. In the Figure - 11 we can easily analyzed the on the surface of the flank fracture is generated.

Conclusion:

In the previous chapter, figure 4 maximum equivalent stresses generated on the surface of the flank and root of the teeth. That two position fracture will start when load applied on flank of the tooth. We derived from calculation in previous chapter the values obtained by Hertz's equation and Ansys agree with each other with a maximum error of 2.81% which is acceptable. It shows that the simulation done in Ansys is compatible and copes up with the hertz equation for this aluminium (2024 –T4) material. Ultimate tensile strength of the aluminium is 310Mpa; beyond that load material is going to fracture. So we applied 400Mpa on the teeth. That

overload draw to tooth failure due to cause of wear, pitting and fracture. That lead to ansys simulation result Figure 10 and 11 we can easily conclude that fracture happen on root of teeth and flank of teeth.

Reference:

[1] Ding Y, Rieger NF. Spalling for mation mechanism for gears. Wear 2003; 254:1307–17.
[2] Batista AC, Dias AM, Lebrun JL, Leflour JC, Inglebert G. Contact fatigue of auto motive gears: evolution and effects of residual stresses introduced by Surface treatments.FatigueFractEngMaterStruct2000;23:217–28.
[3] Aslantaş K, Taşgetiren S. A study of spur gear pitting formation and life prediction.Wear2004;257:1167–75.
[4] Flašker J,FajdigaG,Glodež S, HellenTK. Numerical simulation of surface pitting due to contact loading. IntJFatigue2001;23:599–605.
[5] Šraml M, Flašker J .Computational approach to contact fatigue damage initiation analysis of gear teeth flanks.IntJAdvManufTechnol2007;31: 1066–75.
[6] E.A.P Egbe, Design Analysis and Testing of a Gear Pump, May 2013, 2319-6483.
[7] Litvin FL,FuentesA,Gonzalez-PerezI,CarnevaliL,SepTM. New version of Novikov – Wild haber helical gears: computerized design , simulation of meshing and stressanalysis.ComputMethodsApplMechEng2002;191:5707–40.
[8] Šraml M,Flašker J,Potrč I. Numerical procedure for predicting the rolling contact fatiguecrackinitiation.IntJFatigue2003;25:585–95.
[9] Mao K. Gear tooth contact analysis and its application in the reduction of fatigue wear.Wear2007;262:1281–8.
[10] Osman T, Velex Ph. A model for the simulation of the interactions between dynamic tooth loads and contact fatigue in spur gears.TribolInt2012;46: 84–96.
[11] Sum WS,Williams EJ, Leen SB. Finiteelement, critical-plane, fatigue life prediction of simple and complex contact configurations. IntJFatigue 2005;27:403–16.
[12] Ringsberg JW.Life prediction of rolling contact fatigue crack initiation. IntJ Fatigue2001;23:575–86.
[13] AleksanderK,EwaldM. Are view of critical plane orientations inmultiaxial fatigue failure criteria of metallic materials.IntJFract2005;134:267–304.
[14] Sun JS,LeeKH,LeeHP. Comparison of implicit and explicit finite element methods for dynamic problems.JMaterProcessTechnol2000;105:110–8.
[15] Lin TJ,OuH,LiRf.A finite elementmethodfor3Dstaticanddynamiccontact/ impact analysis of gear drives.ComputMethodsApplMechEng2007;196: 1716–28.
[16] HeinsteinMW,MelloFJ,AttawaySW,LaursenTA. Contact-impact modeling in explicit transient dynamics.ComputMethodsApplMechEng2000;187: 621–40.